

http://journals.tubitak.gov.tr/elektrik/

Turk J Elec Eng & Comp Sci (2015) 23: 813 – 823 © TÜBİTAK doi:10.3906/elk-1210-58

**Research Article** 

# Mechanical fault detection in permanent magnet synchronous motors using equal width discretization-based probability distribution and a neural network model

Mehmet AKAR<sup>1,\*</sup>, Mahmut HEKİM<sup>2</sup>, Umut ORHAN<sup>3</sup>

<sup>1</sup>Mechatronics Engineering Department, Engineering and Natural Sciences Faculty, Gaziosmanpaşa University,

Tokat, Turkey

 $^2\mathrm{Electrical}$  and Electronics Engineering Department, Engineering and Natural Sciences Faculty,

Gaziosmanpaşa University, Tokat, Turkey

<sup>3</sup>Computer Engineering Department, Engineering and Architecture Faculty, Çukurova University, Adana, Turkey

Abstract: This paper focuses on detecting the static eccentricity and bearing faults of a permanent magnet synchronous motor (PMSM) using probability distributions based on equal width discretization (EWD) and a multilayer perceptron neural network (MLPNN) model. In order to achieve this, the PMSM stator current values were measured in the cases of healthy, static eccentricity, and bearing faults for the conditions of three speeds and five loads. The data was discretized into several ranges through the EWD method, the probability distributions were computed according to the number of current values belonging to each range, and these distributions were then used as inputs to the MLPNN model.

We conducted eighteen experiments to evaluate the performance of the proposed model in the detection of faults. The proposed method was very successful in full load and high speed for some experiments. As a result, we showed that the proposed model resulted in a satisfactory classification of accuracy rates.

**Key words:** Permanent magnet synchronous motor (PMSM), eccentricity, bearing faults, equal width discretization (EWD), probability distribution, artificial neural network

## 1. Introduction

Permanent magnet synchronous motors (PMSMs) are more frequently preferred than other motors in industrial applications due to some advantages, such as a high efficiency and power factor, a high power-weight ratio, and a high torque-inertia ratio [1]. In PMSMs, as well as in other rotary machines, periodic maintenance increases motor life, but it is not sufficient for protecting the motor from faults. In recent years, applications engineers and scientists have focused on predictive maintenance instead of periodic maintenance.

The faults that occur in PMSMs can be classified as electrical faults (drive and winding failures), mechanical faults (bearings and eccentricity), and magnetic faults (demagnetization) [2]. Detecting these faults early and taking some precautions will reduce the costs of maintenance and repair as well as increasing operational safety.

Eccentricity faults in electric motors occur because of the unequal air gap between the stator and the rotor. The allowable eccentricity ratio of the manufacturer is between 5% and 10%. However, manufacturers try to reduce as much as possible the amount of eccentricity in order to minimize noise level and the vibration

<sup>\*</sup>Correspondence: mehmet.akar@gop.edu.tr

that occurs in motors. Because of the increase in the amount of eccentricity, rubbing may occur between the rotor and stator windings or the stator core. Eccentricity occurs due to factors such as bending of the motor shaft, incorrect positioning of the motor couplings, and bearing wear [3].

The bearing fault is another mechanical fault that can occur in PMSMs. This fault is usually caused by manufacturing defects, some environmental effects such as high temperature and humidity, and factors such as improper installation and insufficient lubrication [4]. Another reason for bearing faults that can be seen in PMSMs is the motor shaft voltages. While the selection of switching frequency high in the motor drive provides noiseless operation of the motor, it quickly causes defects in the bearings. Shaft voltages induced in the motor shaft over time cause a loss of dielectric of grease on the bearings, which leads to the pulsed currents circulating on the motor shaft. These currents produce deformations on the surface of the bearing [4,5].

Rosero et al. [5] monitored the motor current spectrum for the detection of eccentricity and bearing faults of a PMSM in an experimental study. In another study, the dynamic eccentricity in a PMSM was modeled using the finite element method, and the effects of faults on the current were investigated [6]. Roux et al. [7] monitored the voltage signal applied to the motor terminals as well as the motor current for static and dynamic eccentricity and magnet fracture faults. They carried out the diagnosis of faults using current and voltage spectra. Akar et al. [1] examined the effect of eccentricity faults on the motor current and torque signal in a PMSM. They used the coherence method on the current and torque signals, and revealed the features related to faults. Ebrahimi et al. [8] demonstrated the effect of static, dynamic, and mixed-eccentricity faults on the current spectrum. In another study, Ebrahimi and Faiz [9] monitored the spectrum component of electromagnetic torque signals for the detection of static, dynamic, and mixed eccentricity components. Rosero et al. [10] investigated eccentricity faults in a PMSM operating in the conditions of nonstationary speed using the discrete wavelet transform method. The results obtained from their simulation and experimental study showed that their method can be used successfully for the detection of eccentricity faults. Jongman et al. [11] proposed a new offline method, an inverter-embedded technique, for the detection of demagnetization and eccentricity faults. In their proposed method, the d-axis is excited whenever the motor is stopped using an ac-dc signal, and the variation in the inductance pattern due to demagnetization or eccentricity faults is used to detect these faults. Torregrosa et al. [12] investigated the acoustic variations and torque oscillations caused by partial demagnetization and eccentricity faults occurring in the motor. Ebrahimi and Faiz [13] detected static and dynamic eccentricity faults by monitoring the magnetic field and vibration in a 2D and 3D-modeled PMSM. Li et al. [14] diagnosed the bearing faults occurring in the PMSM by using an independent multiscale principal component analysis and the least squares support vector machine methods together. In another study for the detection of bearing faults, the flux density and bearing friction coefficients were obtained from a robust and dynamic model created for a faulty situation [15]. Akar and Cankaya [16] used current and voltage frequency spectra to detect static eccentricity.

However, most of these studies in the literature focus on the detection of motor faults using the features in the frequency domain. In order to obtain high resolution and accurate results in the frequency domain, a large number of data must be buffered. In this study, our approach is based on the time domain, and therefore the complexity of computation is more suitable for real-time applications. The main advantages of this study are that it does not need extra hardware because of running in time-domain, and the proposed method has a very high classification success rate in the case of maximum class purity. Since frequency domain methods do not need to be used, the study also presents a different point of view for detection of faults in an electrical motor. In the paper, we detect the cases of healthy, static eccentricity and bearing faults in a PMSM by applying the equal width discretization (EWD) method based on probability distributions of datasets of these cases into a multilayer perceptron neural network (MLPNN) model. The EWD-based probability distributions approach was firstly used for the detection of epileptic seizures from EEG signals in a study by Orhan et al. [17]. In the approach, the data were discretized by using the EWD method, the probability distributions for dataset of each case were obtained by finding the number of data points within each discretized interval, and these distributions were used as inputs to MLPNN in order to detect the cases of PMSM fault. A block diagram of the study is shown in Figure 1.

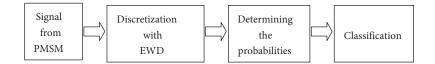


Figure 1. Block diagram of the model proposed in the study.

### 2. Motor current data acquisition and experimental study

The PMSM, whose parameters are given in Table 1, was controlled by the closed loop speed control mode and driven by pulse width modulation (PWM) inverter.

Power	0.82 kW
Voltage	$U_{1N} = 147 V$
Pole pairs	p = 4
Phases	3
Speed	$n_{\rm max} = 9000 \text{ rpm}, n_n = 3000 \text{ rpm}$
Torque	$M_0 = 3 \text{ Nm}, M_n = 2.6 \text{ Nm}$
Current	$I_0 = 3.9 \text{ A}, I_n = 3.5 \text{ A}$

Table 1. PMSM nominal data.

The motor used in the experimental study was driven by a Sinamics CU310DP inverter, and while loading the motor the Foucault brake was used. Depending on the applied voltage applied to the Foucault brake and its drawn current, it produced a load torque between 0 and 20 Nm. Since nominal torque of the motor used in the experiment was 2.6 Nm, the motor could be easily loaded at the desired ratio. In the experimental study, the motors representing three situations (healthy, eccentricity, and bearing faults) in the conditions of low, medium, and nominal speed (600, 1800, and 3000 rpm) and different load levels (0%, 25%, 50%, 75%, and 100%) were operated and motor currents were recorded in a sampling frequency of 8 kHz over 4 s. The data acquisition process was carried out by the interface of the used inverter and its own current sensor. Then, the experimental procedure was repeated for static eccentricity and bearing faults created in the motor artificially. A block diagram of the measurement system of the PMSM and the motor test bench are shown in Figures 2 and 3, respectively [1].

Figure 2 shows a typical PMSM drive with a speed controller, a PWM inverter, speed feedback, and current controllers in the dq-axis (rotor rotating reference frame) [1]. The reference speed command is given  $(\omega_r^*)$ , compared with the actual speed  $(\omega_r)$ , and then a proportional-integral (PI) controller is applied to the speed error signal. The output of the speed controller is a torque reference command, and it is equal to the

q-axis current command  $(T_q^* = i_q^{r*})$ . The reference current is zero for the d-axis  $(i_d^r)$  because rotor excitation is produced by permanent magnets. The outputs of the current controller PI of the dq-axis produce reference command voltages  $V_d^{r*}, V_q^{r*}$  of the dq-axis. These voltages are applied to the PWM inverter to get the voltages, which are the inputs of stator of the PMSM [1]. The air gap between the healthy motor and rotor is around 0.75 mm. The static eccentricity (SE) fault was created by machining out the bearing housing of the motor end bells eccentrically and then placing a 0.3 mm shim to offset the rotor and bearing housing [18]. Thus, an eccentricity fault with a drift of approximately 40% was created in the motor.

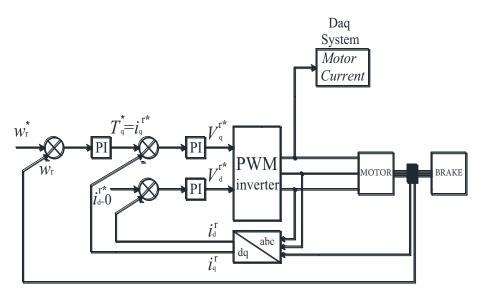


Figure 2. Block diagram for the measurement system.

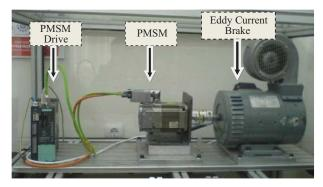


Figure 3. The motor test bench for the experimental study.

A 6204ZZ bearing (the outer and inner diameters are 47 and 20 mm, respectively, the thickness is 14 mm, and its structure is deep groove ball) was used in the experimental study. In order to simulate the possible faults that may occur in bearings, we focused on four different fault types (inner race, outer race, and cage and ball defect). A particular part of the outer cage of the used bearing was cut, and a hole of 4 mm diameter in the inner cage was created so that outer and inner ring faults occurred in the bearing. Similarly, the bearings subjected to the aforementioned faults were obtained by damaging the balls in the bearings and the cage holding the balls. All bearing faults are shown in Figure 4.

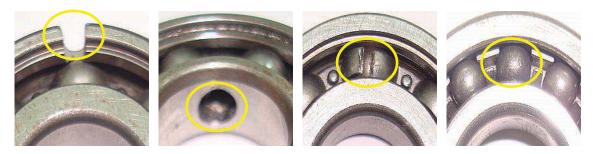


Figure 4. Four bearing faults used in the experimental study.

#### 3. Feature extraction

In this study, the faults of the PMSM were detected by using the probability distributions based on EWD offered in [17]. Discretization methods are very important preprocessing approaches for machine-learning methods since they simplify the information, reduce the computational complexity, and improve the inference algorithm performance. These methods divide a continuous attribute into several ranges, label them with different values, and assign the data points to these labels. They are used for clustering of data points in the noncontinuous digital signals. In general, the effectiveness of a discretization method depends on the algorithm used and the number of ranges. There are many discretization algorithms: equal width, equal frequency [19,20], statistic test [21], information entropy [22–24], and clustering-based discretization [25].

In this study, we used the EWD method to find the probability values in discrete intervals of the current signals of the PMSM. To achieve this, the current signals of the PMSM were divided into k ranges between the minimum  $(v_{min})$  and maximum  $(v_{max})$  values on the amplitude axis. Each range had the width of:

$$w = (v_{\max} - v_{\min})/k \tag{1}$$

and its cutoff points became

$$v_{\min} + w, v_{\min} + 2w, \dots, v_{\min} + (k-1)w$$
 (2)

After the discretization of the current signals using EWD, the probability of the j th signal belonging in the i th range was calculated by

$$P_{ij} = \frac{S_{ij}}{S_j}, i = 1, \dots, k \text{ and } j = 1, \dots, n,$$
 (3)

where  $S_{ij}$  is the number of samples of the *j*th current signal belonging to the *i*th range,  $S_j$  is the number of samples of the *j*th current signal, and *n* is the number of current signals. Figure 5 shows an example of the probability distributions of several current signals taken from the data.

The probability values exist only within the ranges k of 1, 2, and 10 for the healthy dataset; 1, 2, and 4 for the static eccentricity dataset; and 1, 5, 6, 7, and 10 for the bearing faults dataset. These differences in the probability distributions of the signals provide a higher rate of classification successes.

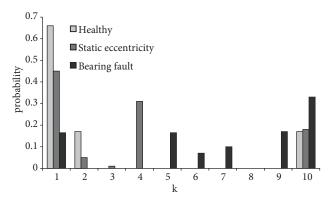


Figure 5. An example of the probability distributions of three current signals at the speed of 3000 rpm for k = 10.

#### 4. Classification

After the feature extraction step, the extracted properties are used as the inputs of a classifier. The classifier used in the study is a MLPNN. The MLPNN has a very classical model structure because it is the beginning of the neural networks. Generally, it has architecture with at least 3 layered neurons, as shown in Figure 6.

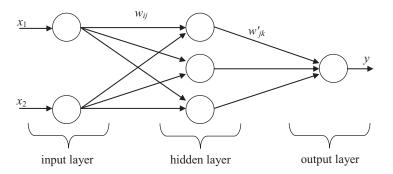


Figure 6. A general architecture for MLPNN with two inputs, three neurons in single hidden layer, and one output.

In the first (input) layer, by multiplying the inputs with some weights, they reach the second (hidden) layer. Each neuron in the hidden layer is the sum of the incoming weighed inputs  $(x_i^* w_{ij})$  and sends the summation into its activation function. Lastly, every neuron in the output layer processes the outputs of the hidden layer as in the hidden layer. Producing an output value by the network is called feed forward. In a feed forward operation, the output value of each neuron is calculated by

$$net_j = f\left(\sum_i x_i w_{ij}\right),\tag{4}$$

where  $x_i$  is the *i*th input,  $w_{ij}$  is the weight between the *i*th input and the *j*th neuron, and *f* is an activation function used to provide nonlinear solutions. The training of the network depends on the error amount in the network output. The most frequently used training algorithm is the generalized delta rule algorithm. It adjusts the weights between neurons with the help of the error in the output. To distribute the output error to weights, the equation below is used:

$$\Delta w(t) = \alpha \Delta w(t-1) - \eta \frac{\partial \left(\frac{1}{2} \left(d(t) - y(t)\right)^2\right)}{\partial w(t)},\tag{5}$$

where y(t) is the computed output, d(t) is the desired output in the dataset,  $\Delta w(t)$  is updating amount of the weight,  $\Delta w(t-1)$  is updating amount of weight in the previous iteration,  $\alpha$  is the momentum coefficient, and  $\eta$  is the learning rate. At first, the energy of the output error is calculated, and then the distribution ratio of the error energy into each weight is determined. In the training procedure, there are some parameters that need to be managed, such as the learning rate and momentum coefficient. Additionally, the activation function for the neurons should be selected according to the problem. Although all of these replaceable parameters can improve the performance of the system, the network should be created again and again because it starts with random initial values.

#### 5. Experimental results

In this study, we detected whether a PMSM is healthy or faulty, and the eccentricity or bearing faults that occur in the PMSM. The healthy and fault datasets of the PMSM were measured in the conditions of 600, 1800, and 3000 rpm speed, and also 0%, 25%, 50%, 75%, and 100% load. Each dataset was discretized by the EWD method for different k values, and their probability distributions for each dataset were computed according to the number of data points within the discretized ranges. For all experiments, the computed probability distributions were used as the inputs to the MLPNN model without any hidden layer. The MLPNN model was used in all experiments since it achieved the best detection successes. This model was trained using the generalized delta rule learning algorithm since it gave better results than other learning algorithms [26]. In the study, MATLAB was chosen as the software development environment that was authorized to manage some parameters such as the momentum coefficient and learning rate. When MATLAB managed these two parameters, it assigned them some initial values (learning rate = 0.01 and momentum coefficient = 0.9). However, according to the gradient descent algorithm, the values change depending on the iteration number. A hyperbolic tangent function was chosen as the activation function for the MLPNN. The model used was validated using a 10- fold cross validation method. The basic aim of the 10-fold cross validation method is to illustrate the generalization of classification success by using available data, and it is one of the most widely used methods for generalizing the results of classifiers. In the experiments, the used data were grouped into 10 subsets. One of the 10 subsets was selected as the test dataset for testing the model, and the others were used for the training and validity datasets. This process was repeated 10 times for each subset. Then the generalized success of the model was computed by averaging 10 results obtained from the test datasets. In the study, we applied the generalized delta rule learning algorithm to our methodology and its number of iterations was fewer than 1000. The proposed method was repeated 100 times for each experiment, and the average of total correct classification (TCC) successes was taken for all experiments. TCC success is the combination of specificity and sensitivity parameters [19,27,28] and it is the proportion of the number of correctly classified decisions (TN +TP) to the number of all cases (TN + FN + TP + FP):

$$TCC = \frac{TN + TP}{TN + FN + TP + FP} \tag{6}$$

Sensitivity is the proportion of the number of true positive (TP) decisions to the number of actually positive cases (TP + FN), and specificity is the proportion of the number of true negative (TN) decisions to the number of actually negative cases (TN+FP):

$$Sensitivity = \frac{TP}{TP + FN}, \text{ and } Specificity = \frac{TN}{TN + FP}, \tag{7}$$

819

where TP is the number of true class events correctly detected as true class, FP is the number of false class events incorrectly detected as true class, TN is the number of false class events correctly detected as false class, and FN is the number of true class events incorrectly detected as false class.

In the study, we implemented 18 different experiments, which are given in detail as follows:

Experiment 1. Detection of bearing faults in the load of 100% and the speed of 3000 rpm.

- Experiment 2. Detection of bearing faults in all loads (0%, 25%, 50%, 75%, and 100%) and the speed of 3000 rpm.
- Experiment 3. Detection of bearing faults in the load of 100% and the speeds of 1800 and 3000 rpm.
- Experiment 4. Detection of bearing faults in all loads (0%, 25%, 50%, 75%, and 100%) and all speeds (600, 1800, and 3000 rpm).
- Experiment 5. Detection of bearing faults in the load of 100% and the speeds of 600, 1800, and 3000 rpm.
- **Experiment 6.** Detection of bearing faults in all loads (0%, 25%, 50%, 75%, and 100%) and all speeds (600, 1800, and 3000 rpm).
- Experiment 7. Detection of eccentricity faults in the load of 100% and the speed of 3000 rpm.
- **Experiment 8.** Detection of eccentricity faults in all loads (0%, 25%, 50%, 75%, and 100%) and the speed of 3000 rpm.
- Experiment 9. Detection of eccentricity faults in the load of 100% and the speeds of 1800 and 3000 rpm.
- Experiment 10. Detection of eccentricity faults in all loads (0%, 25%, 50%, 75%, and 100%) and all speeds (600, 1800, and 3000 rpm).
- Experiment 11. Detection of eccentricity faults in the load of 100% and the speeds of 600, 1800m and 3000 rpm.
- Experiment 12. Detection of eccentricity faults in all loads (0%, 25%, 50%, 75%, and 100%) and all speeds (600, 1800, and 3000 rpm).
- Experiment 13. Detection of all faults (bearing and eccentricity) in the load of 100% and the speed of 3000 rpm.
- Experiment 14. Detection of all faults (bearing and eccentricity) in all loads (0%, 25%, 50%, 75%, and 100%) and the speed of 3000 rpm.
- Experiment 15. Detection of all faults (bearing and eccentricity) in the load of 100% and the speeds of 1800 and 3000 rpm.
- Experiment 16. Detection of all faults (bearing and eccentricity) in all loads (0%, 25%, 50%, 75%, and 100%) and all speeds (600, 1800, and 3000 rpm).
- Experiment 17. Detection of all faults (bearing and eccentricity) in the load of 100% and the speeds of 600, 1800, and 3000 rpm.
- Experiment 18. Detection of all faults (bearing and eccentricity) in all loads (0%, 25%, 50%, 75%, and 100%) and all speeds (600, 1800, and 3000 rpm).

The detection accuracies of the experiments given in detail above are shown in Table 2.

Success $(\%)$
100.00
92.15
92.52
85.18
90.81
73.68
100.00
94.93
96.15
77.00
91.26
65.17
100.00
93.45
92.18
83.75
90.81
72.14

Table 2. The detection results of the experiments in different load and speed conditions.

As seen in Table 2, the tested approach reached 100% in the full load and 3000 rpm speed condition. In contrast, it reached the lowest success rate when all load and speed conditions were used together. As a result, this method provided the highest success in full load condition for the speed of 3000 rpm in the detection of the PMSM faults. As is known, the basic classification process is performed on the 2-class datasets. Many classifier algorithms attain the best results since they are developed for the mentality based on 2-class datasets. Therefore, all the experiments in this study were arranged for 2-class problems. To this end, different class datasets combined in a single class were labeled as the same class dataset. The results of the proposed method for these datasets are illustrated in Table 2. In particular, our approach achieved a high success rate for high speed and full load conditions, which demonstrated that not only is the method capable of very high efficiency but also that the datasets had good class purity. However, because of decreasing class purity, the mixture of a different class of datasets in the other speed and load conditions (0%, 25%, 50%, 75%, and 100%) gradually decreased the classification successes. These results showed that the proposed method is suitable for the classification of PMSM faults in high speed and full load conditions.

### 6. Conclusions

In this paper, we used EWD-based probability distributions of the dataset measured from a PMSM and a MLPNN classifier in the detection of eccentricity and bearing faults. We implemented 18 experiments in different load and speed conditions to evaluate the performance of the proposed model in the detection of the faults. In the experiments, the classifier model achieved a detection success of 100% for the full load condition at the speed of 3000 rpm in the detection of PMSM faults (bearing, eccentricity, and both of them together), while it achieved the lowest success rate when all load and speed conditions were used together. One of the most important advantages of the presented model is that it does not require any additional cost for the user since there are current sensors already available in inverter-driven systems. In addition to their driver ability, the abilities of motor monitoring and fault detection can be given to the inverter by means of additional

software, without any extra hardware requirements. As a result, we showed that the proposed model resulted in satisfactory detection accuracies. Therefore, we suggest that the model used in this study can be used as a diagnostic decision support mechanism in the detection of PMSM faults.

#### References

- M. Akar, S. Taskın, S. Seker, I. Cankaya, "Detection of static eccentricity for permanent magnet synchronous motors using the coherence analysis", Turkish Journal of Electrical Engineering and Computer Sciences, Vol. 18, pp. 963–974, 2010.
- [2] M.B. Ebrahimi, J. Faiz, M.J. Roshtkhari, "Static, dynamic and mixed eccentricity fault diagnosis in permanent magnet synchronous motors", IEEE Transactions on Industrial Electronics, Vol. 56, pp. 4727–4739, 2009.
- [3] P. Vas, Parameter Estimation, Condition Monitoring, and Diagnosis of Electrical Machines. Clarendon Press, Oxford, 1993.
- [4] M. Akar, "Mechanical fault diagnosis in the permanent magnet synchronous motor with artificial intelligence techniques" (in Turkish), PhD Thesis, University of Sakarya, p. 66, 2009.
- [5] J. Rosero, J. Cusido, A. Garcia, J. Ortega, L. Romeral, "Broken bearings and eccentricity fault detection for a permanent magnet synchronous motor", The 32nd Annual Conference of the IEEE Industrial Electronics Society, France, pp. 964–969, 2006.
- [6] M.B. Ebrahimi, J. Faiz, M.J. Roshtkhari, A.Z. Nejhad, "Static eccentricity fault diagnosis in permanent magnet synchronous motor using time stepping finite element method", IEEE Transactions on Magnetics, Vol. 44, pp. 4297–4300, 2008.
- [7] W. Roux, R.G. Harley, T.G. Habetler, "Detecting rotor faults in low power permanent magnet synchronous machines", IEEE Transactions on Power Electronics, Vol. 22, pp. 322–328, 2007.
- [8] M.B. Ebrahimi, J. Faiz, M.J. Roshtkhari, "Static, dynamic and mixed eccentricity fault diagnosis in permanent magnet synchronous motors", IEEE Transactions on Industrial Electronics, Vol. 56, pp. 4727–4739, 2009.
- [9] M.B. Ebrahimi, J. Faiz, "Diagnosis and performance analysis of three phase permanent magnet synchronous motors with static, dynamic and mixed eccentricity", Electric Power Applications, Vol. 4, pp. 53–66, 2010.
- [10] J. Rosero, L. Romeral, G. Rosero, "Detecting eccentricity faults in a PMSM in nonstationary conditions", Ingenieria e Investigacion, Vol. 32, pp. 5–10, 2012.
- [11] H. Jongman, P. Sanguk, H. Doosoo, J. Tae, B.L. Sang, C. Kral, A. Haumer, "Detection and classification of rotor demagnetization and eccentricity faults for PM synchronous motors", IEEE Transactions on Industry Applications, Vol. 48, pp. 923–932, 2012.
- [12] D. Torregrossa, A. Khoobroo, B. Fahimi, "Prediction of acoustic noise and torque pulsation in PM synchronous machines with static eccentricity and partial demagnetization using field reconstruction method", IEEE Transactions on Industrial Electronics, Vol. 59, pp. 934–944, 2012.
- [13] M.B. Ebrahimi, J. Faiz, "Magnetic field and vibration monitoring in permanent magnet synchronous motors under eccentricity fault", IET Electric Power Applications, Vol. 6, pp. 35–45, 2012.
- [14] Z.H. Li, H.F. Mao, J.G. Cui, Y. Zhang, "Motor bearing fault diagnosis based on MSICA-LSSVM", International Conference on Recent Trends in Materials and Mechanical Engineering, Vol. 55–57, pp.747–752, 2011.
- [15] S. Chakraborty, C. Rao, E. Keller, A. Ray, M. Yasar, "Data-driven estimation of multiple fault parameters in permanent magnet synchronous motors", American Control Conference, pp. 204–209, 2009.
- [16] M. Akar, I. Cankaya, "Diagnosis of static eccentricity fault in permanent magnet synchronous motor by on-line monitoring of motor current and voltage", Istanbul University-Journal of Electrical and Electronics Engineering (IU-JEEE), Vol. 9, pp. 959–967, 2009.

- [17] U. Orhan, M. Hekim, M. Ozer, "Epileptic seizure detection using artificial neural network and a new feature extraction approach based on equal width discretization" (in Turkish), Journal of the Faculty of Engineering and Architecture of Gazi University, Vol. 26, pp. 575–580, 2011.
- [18] X. Huang, T.G. Habetler, R.G. Harley, "Detection of rotor eccentricity faults in a closed-loop drive-connected induction motor using an artificial neural network", IEEE Transactions on Power Electronics, Vol. 22, pp. 1552– 1559, 2007.
- [19] U. Orhan, M. Hekim, M. Ozer, "Epileptic seizure detection using probability distribution based on equal frequency discretization", Journal of Medical Systems, Vol. 36, pp. 2219–2224, 2012.
- [20] S. Jiang, X. Li, Q. Zheng, L. Wang, "Approximate equal frequency discretization method", Global Congress on Intelligent Systems, China, pp. 514–518, 2009.
- [21] E.H. Tay, L. Shen, "A modified Chi2 algorithm for discretization", IEEE Transactions on Knowledge and Data Engineering, Vol. 14, pp. 666–670, 2002.
- [22] C.H. Lee, "A Hellinger-based discretization method for numeric attributes in classification learning", Knowledge-Based Systems, Vol. 20, pp. 419–425, 2007.
- [23] U.M. Fayyad, K.B. Irani, "Multi-interval discretization of continuous valued attributes for classification learning", Proceedings of the 13th International Joint Conference on Artificial Intelligence, France, pp. 1022–1029, 1993.
- [24] E.J. Clarke, B.A. Braton, "Entropy and MDL discretization of continuous variables for Bayesian belief networks", International Journal of Intelligence Systems, Vol. 15, pp. 61–92, 2000.
- [25] J. Xi, W.M. Ouyang, "Clustering based algorithm for best discretizing continuous valued attributes", Mini-micro systems, Vol. 21, pp. 1025–1027, 2000.
- [26] B. Karlik, A.V. Olgac, "Performance analysis of various activation functions in generalized MLP architectures of neural networks", International Journal of Artificial Intelligence and Expert Systems, Vol. 1(4), pp. 111–122, 2011.
- [27] U. Orhan, M. Hekim, M. Ozer, "EEG signals classification using the K-means clustering and a multilayer perceptron neural network model", Expert Systems with Applications, Vol. 38, pp. 13475–13481, 2011.
- [28] U. Orhan, M. Hekim, M. Ozer, I. Provaznik, "Epilepsy diagnosis using probability density functions of EEG signals", International Symposium on Innovations in Intelligent Systems and Applications, Turkey, pp. 626–630, 2011.